Mineralocorticoid Receptor Antagonism Attenuates Vascular Apoptosis and Injury via Rescuing Protein Kinase B Activation

Yongzhong Wei, Adam T. Whaley-Connell, Javad Habibi, Jenna Rehmer, Nathan Rehmer, Kamlesh Patel, Melvin Hayden, Vincent DeMarco, Carlos M. Ferrario, Jamal A. Ibdah and James R. Sowers

Hypertension 2009;53;158-165; originally published online Dec 29, 2008;
DOI: 10.1161/HYPERTENSIONAHA.108.121954
Hypertension is published by the American Heart Association. 7272 Greenville Avenue, Dallas, TX 72514
 Print ISSN: 0194-911X. Online ISSN: 1524-4563

Mineralocorticoid Receptor Antagonism Attenuates Vascular Apoptosis and Injury via Rescuing Protein Kinase B Activation

Yongzhong Wei, Adam T. Whaley-Connell, Javad Habibi, Jenna Rehmer, Nathan Rehmer, Kamlesh Patel, Melvin Hayden, Vincent DeMarco, Carlos M. Ferrario, Jamal A. Ibdah, James R. Sowers

Abstract—Emerging evidence indicates that mineralocorticoid receptor (MR) blockade reduces the risk of cardiovascular events beyond those predicted by its blood pressure–lowering actions; however, the underlying mechanisms remain unclear. To investigate whether protection elicited by MR blockade is through attenuation of vascular apoptosis and injury, independently of blood pressure lowering, we administered a low dose of the MR antagonist spironolactone or vehicle for 21 days to hypertensive transgenic Ren2 rats with elevated plasma aldosterone levels. Although Ren2 rats developed higher systolic blood pressures compared with Sprague-Dawley littermates, low-dose spironolactone treatment did not reduce systolic blood pressure compared with untreated Ren2 rats. Ren2 rats exhibited vascular injury as evidenced by increased apoptosis, hemidesmosome-like structure loss, mitochondrial abnormalities, and lipid accumulation compared with Sprague-Dawley rats, and these abnormalities were attenuated by MR antagonism. Protein kinase B activation is critical to vascular homeostasis via regulation of cell survival and expression of apoptotic genes. Protein kinase B serine^{473} phosphorylation was impaired in Ren2 aortas and restored with MR antagonism. In vivo MR antagonist treatment promoted antiapoptotic effects by increasing phosphorylation of BAD serine^{136} and expression of Bcl-2 and Bcl-xL, decreasing cytochrome *c* release and BAD expression, and suppressing caspase-3 activation. Furthermore, MR antagonism substantially reduced the elevated NADPH oxidase activity and lipid peroxidation, expression of angiotensin II, angiotensin type 1 receptor, and MR in Ren2 vasculature. These results demonstrate that MR antagonism protects the vasculature from aldosterone-induced vascular apoptosis and structural injury via rescuing protein kinase B activation, independent of blood pressure effects. **(*Hypertension*. 2009;53:158-165.)**

Key Words: aldosterone ■ oxidative stress ■ Akt activation ■ vascular apoptosis and injury

Clinical studies indicate that mineralocorticoid receptor (MR) blockade exerts beneficial effects on cardiovascular events beyond those predicted by its blood pressure (BP)–lowering actions.[1–4] Experimental evidence further suggests that aldosterone exerts direct adverse effects on the vasculature, contributing to vascular injury and remodeling.[5–8] However, the underlying molecular mechanisms by which signaling through the MR elicits these deleterious vascular effects independently of BP increases remain to be elucidated.

Apoptosis has been implicated in the pathogenesis of vascular injury and remodeling, leading to development of vascular disease.[9–11] Excessive apoptosis contributes to vascular cell loss, impairs endothelium-dependent vasorelaxation, promotes inflammation, and enhances procoagulant activity.[12] Evidence indicates that increased hemodynamic and mechanical forces contribute to vascular cell apoptosis.[13] Aldosterone further promotes apoptosis in cultured endothelial cells (ECs),[14] implying a direct or indirect role in the pathogenesis of vascular apoptosis and injury. The extent to which the vascular protective effects of MR blockade in vivo are the direct result of attenuation of apoptosis independent of BP reductions, and the molecular mechanisms involved in this protective effect, remains unclear.

Protein kinase B (Akt), a serine (Ser)/threonine protein kinase, plays a critical role in inhibiting cardiovascular cell apoptosis, including ECs.[15] Akt Ser^{473} residue phosphorylation exerts antiapoptotic actions through several mechanisms, including regulation of mitochondrial membrane integrity, suppression of proapoptotic signaling, and enhancement of antiapoptotic molecule expression. BAD, a proapoptotic molecule, initiates apoptosis by binding to the antiapoptotic

Received August 21, 2008; first decision September 9, 2008; revision accepted December 7, 2008.

From the Departments of Medicine and Physiology (Y.W., A.T.W.-C., J.H., J.R., N.R., K.P., M.H., V.D., J.A.I., J.R.S.), Diabetes and Cardiovascular Center of Excellence (Y.W., A.T.W.-C., J.H., J.R., N.R., M.H., V.D., J.R.S.), University of Missouri, Columbia; Harry S. Truman VA Medical Center (J.A.I., J.R.S.), Columbia, Mo; and Hypertension and Vascular Disease Center (C.M.F.), Wake Forest University School of Medicine, Winston-Salem, NC.

Correspondence to James R. Sowers, MD, Professor of Medicine, Pharmacology, and Physiology, Director of the Diabetes and Cardiovascular Center of Excellence, University of Missouri–Columbia, D109 Diabetes Center HSC, 1 Hospital Dr, Columbia, MO 65212. E-mail sowersj@health.missouri.edu

Hypertension **is available at http://hyper.ahajournals.org** **DOI: 10.1161/HYPERTENSIONAHA.108.121954**

molecules Bcl-xL and Bcl-2 on the outer mitochondrial membrane, causing cytochorome *c* release into the cytosol.[16–18] Akt phosphorylates BAD on Ser^{136}, which prevents BAD from binding to Bcl-xL and Bcl-2, thus preventing the proapoptotic function of BAD.[16] Akt also plays an important role in cell metabolism and regulation of various vascular functions. Indeed, Akt knockout mice exhibit various vascular abnormalities, including increased apoptosis and lipid accumulation.[19]

It was reported recently that in vitro aldosterone treatment impairs Akt activation in vascular smooth muscle cells (SMCs).[20] Accordingly, we hypothesized that aldosterone, acting through MR stimulation, suppresses vascular Akt activation, which, in turn, promotes vascular apoptosis and lipid accumulation and injury. We further hypothesized that the effects of aldosterone could be attenuated by in vivo treatment with the MR antagonist spironolactone. To this end, we used the transgenic Ren2 rat model, which overexpresses the mouse renin gene in the adrenal glomerulosa, resulting in elevated aldosterone plasma levels.[21,22] Furthermore, to assess BP-independent effects of MR antagonism on the vasculature protection, we used a dose of spironolactone, which does not reduce systolic BP (SBP) in hypertensive Ren2 rats.[23]

Materials and Methods

Details of the materials and methods can be found in an online supplement available at http://www.hypertension.aha.org.

Animals and Treatments

Animal procedures were followed by the University of Missouri Animal Care and Use Committee and National Institutes of Health guidelines. Six- to 7-week-old male transgenic heterozygous (+/−) Ren2 rats and Sprague-Dawley (SD) littermates were assigned randomly to SD vehicle–treated, Ren2 vehicle–treated controls (Ren2-C) and Ren2 spironolactone groups (6 to 7 rats per group). Rats were implanted with a subcutaneous time-release, matrix-driven delivery pellet containing either spironolactone (5 mg; 0.24 mg/day) or vehicle for 21 days.[23]

Systolic BP

SBP was measured before and after treatment.[23]

Aorta Dissection and Protein Extraction

Thoracic aorta was used in this study.

NADPH Oxidase Activity Assay

NADPH oxidase activity was measured as described previously.[24]

Western Blot Analysis

4-Hydroxy-nonenal (4-HNE), 3-nitrotyrosin, cytochrome *c*, BAD, BAD Ser^{136}, total-Akt, Akt Ser^{473} phosphorylation, caspase-3, and angiotensin type 1 receptor (AT_1R) were analyzed by Western blot.

Immunofluorescence

Paraffin and cryostat sections were used for immunohistochemistry with the following antibodies against: BAD Ser^{136}, Bcl-2, Bcl-xL, Akt Ser^{473}, Akt threonine^{308}, angiotensin II (Ang II), AT_1R, MR, Nox2, Rac1, $p67^{phox}$, or 3-nitrotyrosine, respectively.

Evaluation of Apoptotic Cell Death by TUNEL

TUNEL assay was performed using In Situ Cell Death Detection Kit (Roche Diagnostics).

Oil Red O Staining

Oil Red O staining was performed on frozen aortic sections.

Transmission Electronic Microscopy

The ultrastructural changes of vasculature were examined by transmission electronic microscopy (TEM).

Statistical Analysis

All data are reported as the means±SEM. Dunnett's test or Student *t* test was used to determine the significance among groups. A value of $P<0.05$ was considered statistically significant.

Results

Spironolactone Treatment Did not Influence SBPs in Ren2 Rats

Ren2 rats at 6 to 7 weeks of age had higher SBP than SD controls (SD-C; $P<0.01$), which increased further at 9 to 10 weeks of age ($P<0.01$). Spironolactone treatment did not reduce SBP compared with untreated Ren2 rats ($P>0.05$; Figure 1A). Interestingly, despite not reducing SBP, spironolactone treatment attenuated the increases in medial wall thickness observed in untreated Ren2 rats (Figure 1B).

Spironolactone Treatment Attenuated Vascular Activity of Renin-Angiotensin-Aldosterone System in Ren2 Rats

To determine whether spironolactone treatment affects aortic tissue renin-angiotensin-aldosterone system activity, expression of MR, Ang II, and AT_1R was analyzed using immunohistochemistry and Western blot. Ren2 aortas exhibited increased MR expression (Figure 1C), Ang II (Figure 1D and 1E) and AT_1R (Figure 1F and 1G) compared with SD, all attenuated with spironolactone treatment.

Spironolactone Treatment Attenuated Vascular Oxidative Stress in Ren2 Rats

Lipid peroxidation was determined by measuring 4-HNE and 3-nitrotyrosine by Western blot (Figure 2A and 2B) and immunohistochemistry (data not shown). There was a significant increase of 4-HNE (Figure 2A) and 3-nitrotyrosine (Figure 2B) in Ren2 aortic tissues compared with SD, and spironolactone treatment decreased 4-HNE and 3-nitrotyrosine levels in Ren2 aortas (Figure 2A and 2B). To determine whether attenuation of lipid peroxidation by spironolactone treatment in Ren2 aortas is attributable to suppression of NADPH oxidase activation, the activity and subunit expression of this enzyme were measured. Ren2 aortas exhibited greater activity (Figure 2C) and increased expression of Nox2, Rac1, and $p67^{phox}$ subunits (Figure 2D, 2E, and 2F, respectively) of NADPH oxidase compared with SD, attenuated with spironolactone treatment compared with untreated Ren2-C (Figure 2C through 2F).

Spironolactone Treatment Improved Vascular Akt Activation in Ren2 Rats

Akt Ser^{473} phosphorylation was significantly decreased in Ren2 aortas compared with SD ($P<0.05$), which was improved with spironolactone treatment compared with untreated Ren2 aortas ($P<0.05$; Figure 3A). Immunostaining intensities for Akt Ser^{473} and theorine^{308} were decreased in Ren2 aortic sections compared with SD and similarly improved with spironolactone treatment (Figure 3B and 3C).

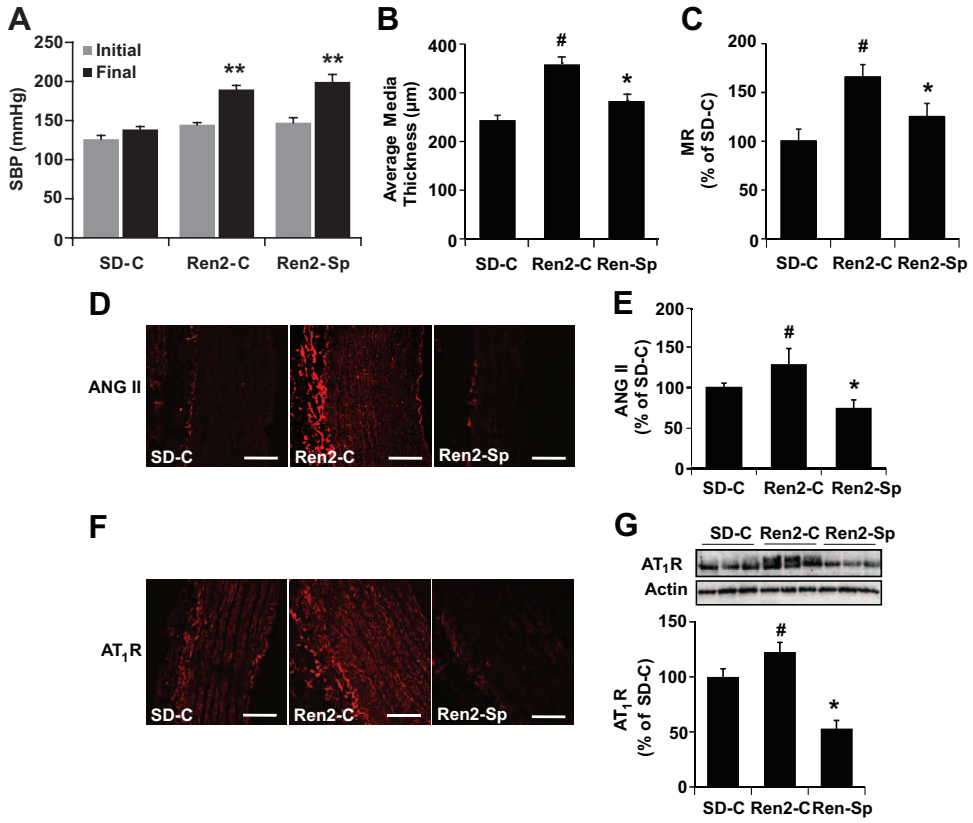

Figure 1. MR blockade did not influence SBP but attenuated aortic tissue hypertrophy and renin-angiotensin-aldosterone system activity in Ren2 rats. A, SBP was measured at the initial and final stages of experiment. B, Average aortic media thickness. C, Average gray scale intensities of immunostaining for MR. D, Representative immunostaining images for Ang II (ANG II). E, Average gray scale intensities of immunostaining for Ang II. F, Representative immunostaining images for AT_1R. G, Representative Western blot for AT_1R (top; 50 kDa); bar graph showed the band densitometry analysis (bottom). The results are means±SEM from 6 to 7 rats per group. $^{**}P<0.01$ vs age-matched SD-C (at the final stage); there was no significant difference in SBP between spironolactone-treated Ren2 (Ren2-Sp) and Ren2-C (at the final stage). #$P<0.05$ vs SD-C; $^{*}P<0.05$ vs Ren2-C. D and F, Magnification ×400; bar=50 μm.

Spironolactone Treatment Enhanced BAD Ser^{136} Phosphorylation and Antiapoptotic Protein Expression in Ren2 Rats

Expression of BAD Ser^{136} phosphorylation (Figure 4A and 4B), Bcl-2 (Figure 4C), and Bcl-xL (Figure 4D) was decreased in Ren2 aortas compared with SD and improved with spironolactone treatment compared with untreated Ren2 aortas (Figure 4A through 4D). In contrast, BAD expression was significantly increased in Ren2 aortas compared with SD, and attenuated with spironolactone treatment (Figure 4E).

Spironolactone Treatment Attenuated Vascular Mitochondrial Abnormalities and Cytochrome *c* Release in Ren2 Rats

Mitochondrial damage impairs mitochondrial membrane integrity and causes cytochrome *c* release into cytosol, contributing to apoptosis.[17,18,25] Mitochondria are vulnerable to damage by a variety of pathological insults, including reactive oxygen species.[26] Ultrastructural analysis demonstrated that Ren2 vascular mitochondria displayed abnormalities, including swelling, cristae disruption, and reduced matrix density compared with SD vasculature, and these abnormalities were partly corrected after spironolactone treatment (Figure 5A). Double immunostaining for mitochondrial complex 4 subunit 1 and cytochrome *c* showed that there was a diffuse staining pattern for cytochrome *c*, which did not colocalize with mitochondrial complex 4 subunit 1 staining in Ren2 aortas compared with SD (Figure 5B). These alterations in cytochrome *c* staining in Ren2 aortic tissue were partly corrected with spironolactone treatment (Figure 5B). Western blot analysis showed that there was increased cytochrome *c* release into cytosol in Ren2 aortic tissues compared with SD, which was attenuated with spironolactone treatment (Figure 5C).

Spironolactone Treatment Attenuated Vascular Apoptosis in Ren2 Rats

TEM ultrastructural analysis demonstrated apoptotic cells with nuclear condensation, clumping, and loss of cytosolic and plasma membrane integrity in ECs and SMCs in Ren2 arteries (Figure 6A). TUNEL staining showed that there were apoptotic ECs and SMCs in Ren2 aortic sections (Figure 6B). As shown in Figure 6C, there was 2.6-fold increase of apoptotic cells in Ren2 aortic sections compared with SD ($P<0.01$), which was substantially reduced after spironolactone treatment ($P<0.05$). Immunoblot analysis further confirmed this observation that Ren2 vasculatures exhibited increased activated caspase-3, a key enzyme in apoptosis pathways, compared with SD-C ($P<0.05$), which were attenuated after spironolactone treatment ($P<0.05$) (Figure 6D).

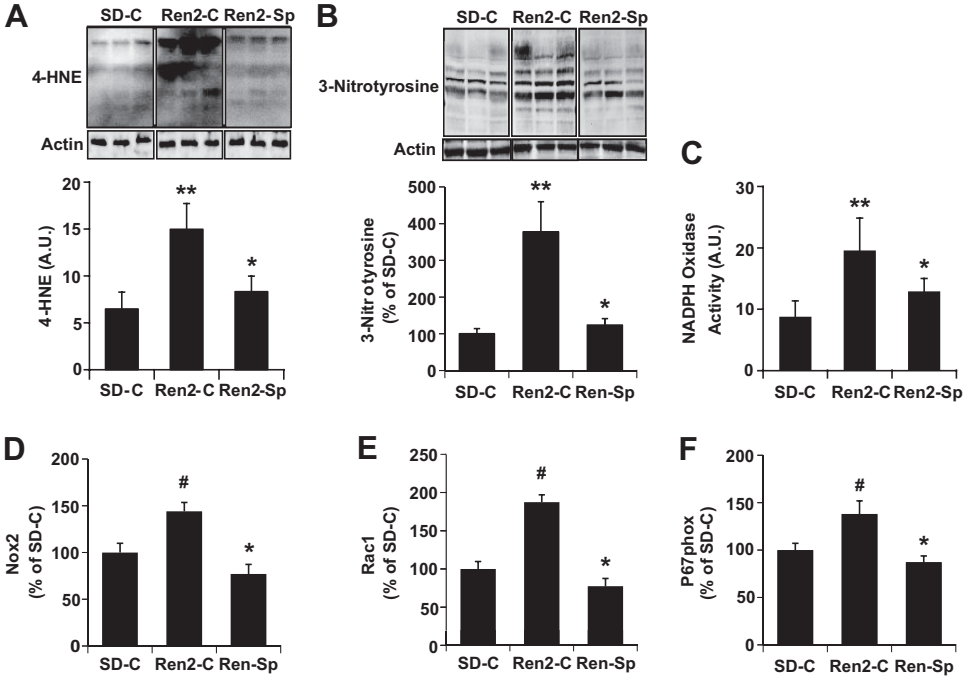

Figure 2. MR blockade attenuated vascular lipid peroxidation in Ren2 rats. A, Representative Western blot for 4-HNE (top; multiple bands); bar graph showed a quantitative densitometry analysis of 4-HNE bands (bottom). A.U. indicates arbitrary units. B, Representative Western blot for 3-nitrotyrosine (top; multiple bands); bar graph showed the band densitometry analysis (bottom). C, NADPH oxidase activity. D through F, Average gray scale intensities of immunostaining for Nox2, Rac1, and $p67^{phox}$. The results are means±SEM; 6 to 7 rats per group. Ren2-Sp indicates spironolactone-treated rats. $^{**}P<0.01$ vs SD-C; #$P<0.05$ vs SD-C; $^{*}P<0.05$ vs Ren2-C.

Spironolactone Treatment Attenuated Vascular Ultrastructural Abnormalities in Ren2 Rats

Evidence suggests that activated caspase-3 cleaves integrin $\beta 4$, a key component of hemidesmosomes, promoting apoptosis.[27] TEM showed that Ren2 vasculatures exhibited hemidesmosome-like structure (endothelial basal adhesion plaque) loss, which was attenuated with spironolactone treatment (Figure 7A). The basal adhesion plaques that promote adhesion of the endothelium to the internal elastic matrix were structurally similar to hemidesmosomes responsible for epithelial cell–matrix attachments, and they are thus referred to as hemidesmosome-like structures. Hemidesmosome-like structure loss disrupts cell–matrix (elastin of the internal elastic lamina) interaction and adhesion, which might have contributed to increased vascular EC apoptosis observed in Ren2 vasculatures. A recent study suggests that aldosterone stimulates migration of vascular SMCs.[28] Ren2 vasculatures also displayed SMC migration into intimal layer and internal elastic lamina disruption compared with SD vasculatures and were attenuated with spironolactone treatment (data not shown).

Spironolactone Treatment Attenuated Vascular Lipid Accumulation in Ren2

Lipid accumulation in vasculature is also a characteristic of vascular injury/maladaptation.[29,30] Impaired Akt activation and damaged mitochondria have been suggested to promote vascular lipid accumulation.[19] Oil red O staining indicated increased lipid accumulation in media (Figure 7B) and ECs (data not shown) in Ren2 aortas compared with SD; this observation was supported by TEM (Figure 7C). Lipid accumulation in Ren2 aortas was attenuated with spironolactone treatment (Figure 7B and 7C).

Discussion

Evidence suggests that MR blockade exerts a protective effects on cardiovascular outcomes.[1–3] Although increased

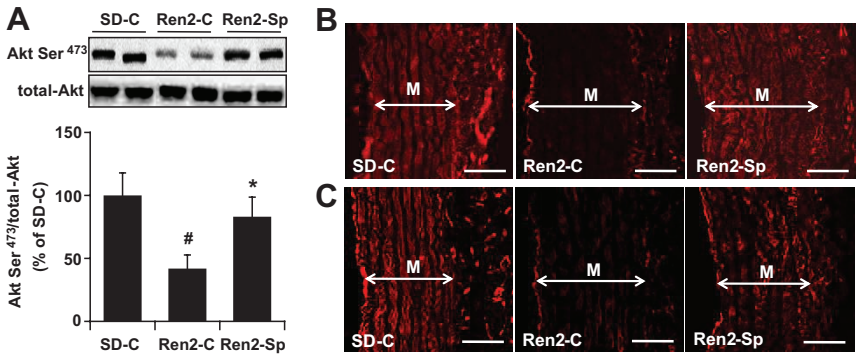

Figure 3. MR blockade improved Akt activation in Ren2 rats. A, Representative Western blot for Akt Ser^{473} (60 kDa) and total Akt (60 kDa; top); bar graph showed a ratio of Akt Ser^{473}/total Akt for the band densitometry analysis (bottom). B, Representative immunostaining images for Akt Ser^{473}. C, Representative immunostaining images for Akt theorine[308]. The results are mean±SEM from 6 rats for each group. #$P<0.05$ vs SD-C; $^{*}P<0.05$ vs Ren2-C. Ren2-Sp indicates spironolactone-treated rats; M, media. Magnification ×400; bar=50 μm.

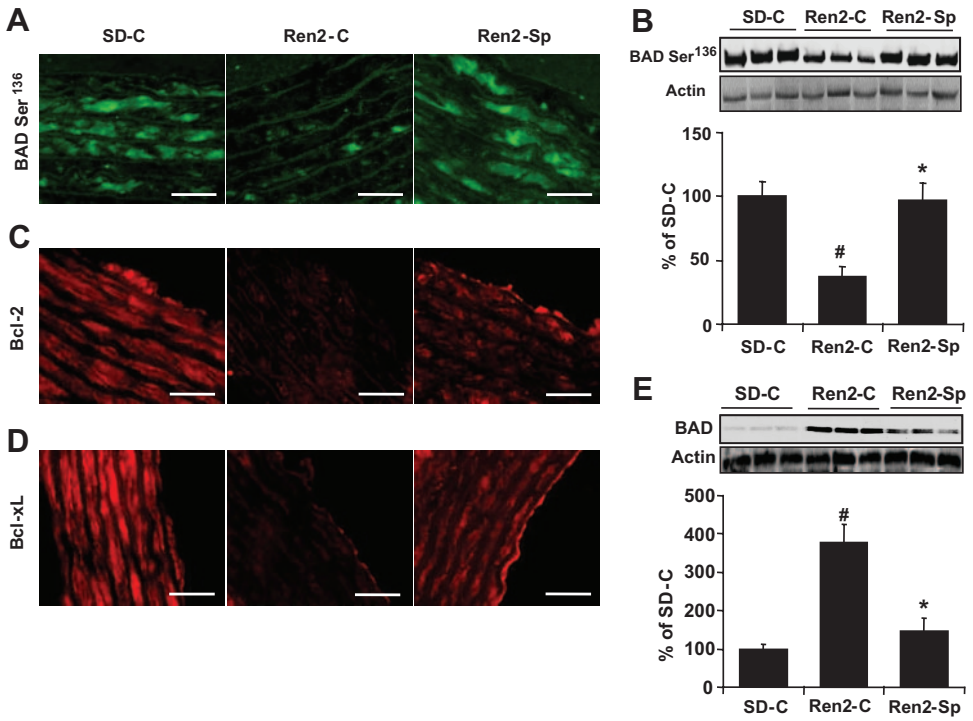

Figure 4. MR blockade enhanced BAD Ser[136] phosphorylation and expression of Bcl-xL and Bcl-2, and suppressed BAD expression in Ren2 rats. A, Representative immunostaining images for BAD Ser[136]. B, Representative Western blot for BAD Ser[136] (top; 25 kDa); bar graph showed the band densitometry analysis (bottom). C, Representative immunostaining images for Bcl-2. D, Representative immunostaining images for Bcl-xL. E, Representative Western blot for BAD (top; 25 kDa); bar graph showed the band densitometry analysis (bottom). A, C, and D, Magnification ×400; bar=50 μm. The results are mean±SEM from 6 rats for each group. Ren2-Sp indicates spironolactone-treated rats. #$P<0.05$ vs SD-C; *$P<0.05$ vs Ren2-C.

BP mediated by aldosterone causes vascular injury, recent evidence suggests that aldosterone also exerts direct maladaptive effects on the vasculature.[5,7,31] Although vascular injury is a key step for initiation and progression of cardiovascular diseases, little is known regarding the molecular mechanisms underlying aldosterone-induced deleterious effects on the vasculature. The current investigation provides novel findings that MR blockade delivers a direct protection against aldosterone-induced vascular apoptosis, mitochondrial damage, lipid accumulation, and endothelial basal hemidesmosome-like structure loss via rescuing Akt activation, independent of BP/hemodynamic actions.

The transgenic Ren2 rat overexpresses the mouse renin gene in the adrenal glomerulosa, resulting in increased tissue Ang II and elevated plasma aldosterone levels. We observed previously that AT_1R blockade[32] and treatment with high doses of spironolactone (our unpublished observation, 2007) significantly decrease BP in Ren2 rats, suggesting that Ang II and aldosterone are involved in hypertension development in Ren2 rats. We report here that Ren2 aortas exhibit increased

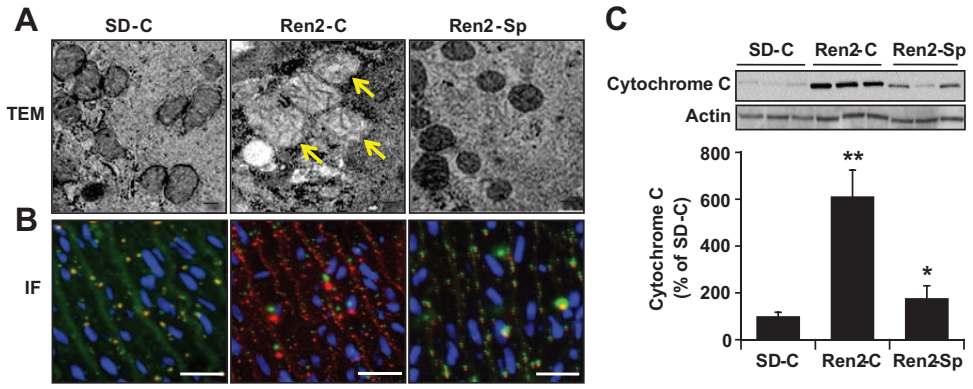

Figure 5. MR blockade attenuated vascular cell mitochondria injury and cytochrome *c* release in the Ren2 rats. A, Representative TEM images showed abnormal mitochondria with swollen and reduced matrix density in Ren2 rats (yellow arrow), magnification ×12 000; bar=100 nm. B, Representative double immunofluorescent (IF) staining for MTCO1 (green), cytochrome *c* (red), overlap (yellow), and nuclei (DAPI; blue), magnification ×400; bar=50 μm. C, Representative Western blot for cytochrome *c* in cytosolic fractions (top; 15 kDa) and bar graph shows a quantitative densitometry of cytochrome *c* bands (bottom). Ren2-Sp indicates spironolactone-treated rats. The results are means±SEM; 6 rats per group. **$P<0.01$ vs SD-C; *$P<0.05$ vs Ren2-C.

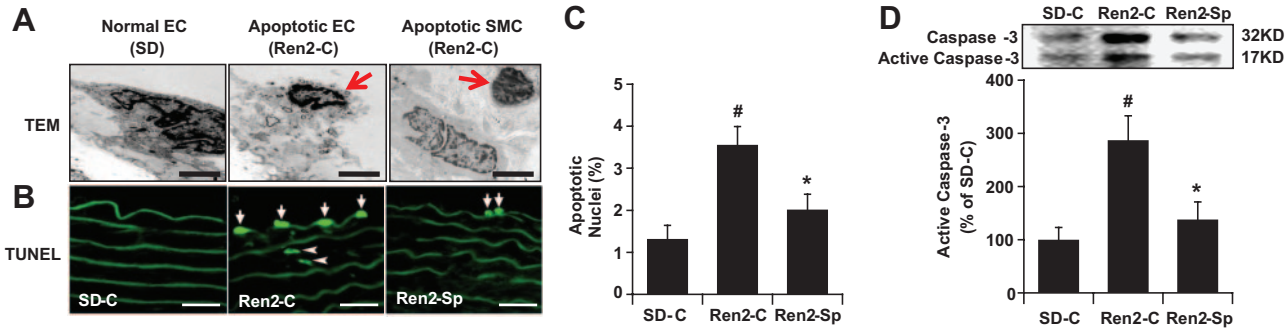

Figure 6. MR blockade attenuated vascular cell apoptosis in Ren2 rats. A, Representative TEM images showed apoptotic ECs and SMCs from Ren2 rats, magnification ×6000; bar=0.5 μm. B, Representative TUNEL staining photomicrographs showed vascular apoptotic ECs (arrow) and SMCs (arrowhead), magnification ×400; bar=50 μm. Ren2-Sp indicates spironolactone-treated rats. C, Bar graph shows ratio of TUNEL-positive cell/total cells×100%. D, Activated caspase-3 were analyzed by immunoblot; the graph indicated quantitative densitometry analysis. The results are mean±SEM from 3 sections per animal and 6 rats per group. #$P<0.05$ compared with SD-C; *$P<0.05$ compared with Ren2-C.

aortic tissue levels of Ang II, AT_1R, and MR compared with SD. In the present investigation, we used a very low dose of spironolactone to determine whether MR blockade provides direct vasculature protection independent of BP reduction. The measurement of BP by the tail-cuff method may be a limitation in the current study; nevertheless, low-dose spironolactone treatment reduced aortic tissue levels of Ang II, AT_1R, and MR in Ren2 rats. This is consistent with a recent report that spironolactone in higher doses (50 mg/kg per day) reduces the expression of angiotensin converting enzyme, MR, and aldosterone synthase in streptozotocin-induced diabetic kidney.[33] Our data suggest that MR blockade exerts direct protection from vascular injury, in part, through modulation of Ang II, AT_1R, and MR expression in the Ren2 rat model.

Apoptosis has been implicated as an important mechanism in the pathogenesis of vascular disease.[11,34] Apoptosis promotes vascular cell loss. Apoptosis also induces vascular dysfunction, inflammatory cell infiltration, and lipid accumulation, all of which further aggravate vascular cell apoptosis.[11,12] There were significantly increased apoptotic endothelial and SMC deaths detected by TUNEL assay in Ren2 aortas compared with SD aortas, and these differences were substantially decreased after spironolactone treatment (Figure 4). TUNEL assay is a sensitive and standard technique for studying apoptosis in various tissues. However, TUNEL assay may also recognize cells undergoing DNA repair.[35,36] We further corroborated our TUNEL results with morphological characterization of apoptosis by light microscope and TEM as well as DNA electrophoresis. Both light microscopic (data not shown) and TEM findings (Figure 4) indicated that there were more apoptotic nuclei in Ren2 aortic sections compared with SD, and this difference was attenuated with spironolactone treatment (data not shown). Furthermore, DNA electrophoresis showed that there were increased DNA fragmentations in Ren2 aortic tissue compared with SD, attenuated with spironolactone treatment (data not shown). In addition, active caspase-3, a more specific indicator for cells going to apoptosis, was increased in Ren2 aortic tissues compared with SD, abrogated after spironolactone treatment (Figure 4). Collectively, these novel data support the notion that MR antagonism exerts a direct protective role in vascular tissue exposed to high levels of circulating aldosterone. Our results are consistent with recent reports that aldosterone induces cell apoptosis in cultured ECs,[14] proximal tubular cells,[37] mesangial cells,[38] and cardiac myocytes.[39] In contrast, a recent report indicates that spironolactone induces cell apoptosis in cultured mononuclear cells.[40] Together, these data suggest that the effects of spironolactone on cell apoptosis may be dependent on the cell type and culture conditions. We extend these in vitro observations and report here for the first time that in vivo MR antagonism attenuates vascular cell apoptosis independent of BP-lowering action.

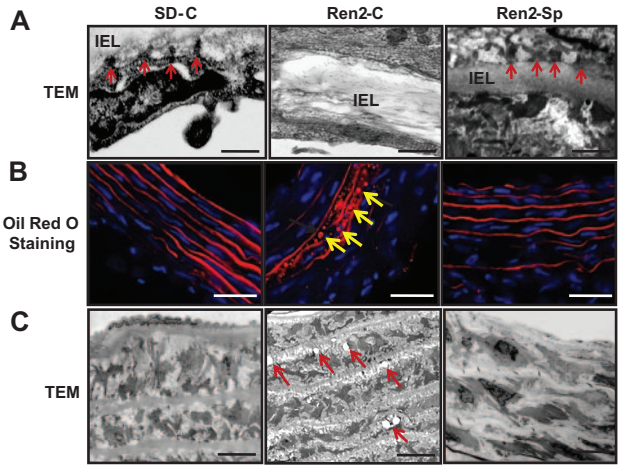

Figure 7. MR blockade attenuated vascular hemidesmosome-like structural loss and lipid accumulation in the Ren2 rats. A, Representative TEM images indicated hemidesmosome-like structures (arrows), IEL (internal elastic lamina), magnification ×12 000; bar=100 nm. B, Representative Oil Red O staining showed lipid droplets in SMCs from Ren2 rats (arrow), magnification ×400; bar=50 μm. C, Representative TEM images showed intracellular lipid vesicles in SMCs (arrow) from Ren2 rats, magnification ×3000; bar=10 μm. Ren2-Sp indicates spironolactone-treated rats.

Our findings also suggest that the vasculature protections by MR blockade are mediated by suppression of oxidative stress and improvement of Akt activation. In this regard, Akt Ser^{473} phosphorylation/activation was dramatically decreased in Ren2 aortas and was substantially improved after spirono-

lactone treatment (Figure 3). Interestingly, immunostaining intensities of Akt Ser[473] phosphorylation on ECs were comparable among SD-C, Ren2-C, and Ren2 spironolactone (data not shown); although immunostaining intensities of Akt threonine[308] phosphorylation in ECs were dramatically decreased in Ren2 aortic sections compared with SD, they were increased with spironolactone treatment (data not shown). Our results are consistent with a recent report that aldosterone impairs Akt activation in cultured vascular SMCs.[20] The increased levels of 4-HNE and 3-nitrotyrosine in Ren2 aortas were markedly decreased with spironolactone treatment (Figure 2). The increased activity and expression of NADPH oxidase observed in Ren2 aortas were abrogated after spironolactone treatment, suggesting that there is MR mediation of NADPH oxidase activation as a source of oxidative stress. Oxidative stress has been shown to inhibit Akt activation in various tissues, including vasculature through direct or indirect actions.[41]

Akt activation is crucial in cell survival[17–19,25] through inhibiting apoptosis by suppressing proapoptotic or enhancing antiapoptotic signal, as well as regulation of mitochondrial membrane integrity and cytochrome *c* release. BAD is a proapoptotic molecule and usually maintained in phosphorylated and sequestered form in the cytosol. When dephosphorylated, BAD migrates into mitochondria, binds to Bcl-2 and Bcl-xL, and releases cytochrome *c* into the cytosol. Akt activation promotes phosphorylation and inactivation of BAD.[17,18] Akt activation increases antiapoptotic molecule expression such as Bcl-2.[17,18] Akt phosphorylation also promotes Akt translocation to the nucleus, where it affects the transcription of target genes and exerts protective activity.[42] Indeed, decreased expression of BAD Ser[136] phosphorylation, Bcl-xL, and Bcl-2 was observed in Ren2 aortas compared with SD and was improved after spironolactone treatment. This was consistent with attenuation of mitochondrial injury and cytochrome *c* release into cytosol in treated Ren2 vasculatures with spironolactone. Our results are also consistent with a recent study that aldosterone treatment enhances dephosphorylation of phosphor–BAD and release of cytochrome *c* into cytosol in cultured mesangial cell.[38] Increased cytochrome *c* in cytosol activates caspase-3, resulting in cell apoptosis. Active caspase-3 has been shown recently to cleave the key component integrin β4 of hemidesmosomes and impair hemidesmosome formation, promoting apoptosis.[27] Ren2 arteries exhibited hemidesmosome-like structural loss, which was preserved by spironolactone treatment; these, together with increased proapoptotic proteins, contribute to increased vascular apoptosis and injury in Ren2 rats.

Akt activation also plays a vital role in regulating cell metabolism, including lipid oxidation. Lipid accumulation is a prominent feature of vascular disease and also an etiologic factor of vascular injury. Indeed, Akt knockout mice display increased vascular lipid accumulation and develop severe vascular injury and atherosclerosis.[19] In this context, there was increased vascular lipid accumulation in Ren2 aortas, abolished by in vivo MR blockade.

In summary, the results of this investigation indicate that elevated aldosterone levels acting via the MR promote NADPH oxidase activation/reactive oxygen species production, which, in turn, impairs Akt activation and consequently causes activation of apoptotic signaling pathways, lead to vascular cell apoptosis, lipid accumulation, and injury.

Perspectives

This investigation provides novel evidence that MR antagonism provides direct protection of vascular cells from apoptosis and injury independent of BP/hemodynamic actions. These protective effects are mediated by improvement of Akt activation and suppression of cell death pathways. These data also demonstrate that there is a potentially distinct therapeutic target mediated via rescuing Akt activation. Finally, these data help us understand some of the molecular mechanisms by which therapy with MR antagonists have provided protection against cardiovascular events in patients at high risk.

Acknowledgments

The authors would like to thank Rebecca Schneider and the University of Missouri Electron Microscope Core for their excellent technique and tissue preparation.

Sources of Funding

This work was supported by National Institutes of Health grant RO1-HL073101–02 and VA Merit 0018 (J.R.S.), VA VISN 15 (A.W.C.), and the Missouri Kidney Program (A.W.C.).

Disclosures

None.

References

1. Pitt B, Zannad F, Remme WJ, Cody R, Castaigne A, Perez A, Palensky J, Wittes J. The effect of spironolactone on morbidity and mortality in patients with severe heart failure. Randomized Aldactone Evaluation Study Investigators. *N Engl J Med*. 1999;341:709–717.
2. Pitt B. Aldosterone blockade in patients with systolic left ventricular dysfunction. *Circulation*. 2003;108:1790–1794.
3. Pitt B, Reichek N, Willenbrock R, Zannad F, Phillips RA, Roniker B, Kleiman J, Krause S, Burns D, Williams GH. Effects of eplerenone, enalapril, and eplerenone/enalapril in patients with essential hypertension and left ventricular hypertrophy: the 4E-left ventricular hypertrophy study. *Circulation*. 2003;108:1831–1838.
4. Gomez-Sanchez CE, Gomez-Sanchez EP. Role of central mineralocorticoid receptors in cardiovascular disease. *Curr Hypertens Rep*. 2001;3:263–269.
5. Brown NJ. Aldosterone and vascular inflammation. *Hypertension*. 2008;51:161–167.
6. Rocha R, Rudolph AE, Frierdich GE, Nachowiak DA, Kekec BK, Blomme EA, McMahon EG, Delyani JA. Aldosterone induces a vascular inflammatory phenotype in the rat heart. *Am J Physiol Heart Circ Physiol*. 2002;283:H1802–H1810.
7. Schiffrin EL. Effects of aldosterone on the vasculature. *Hypertension*. 2006;47:312–318.
8. Martinez DV, Rocha R, Matsumura M, Oestreicher E, Ochoa-Maya M, Roubsanthisuk W, Williams GH, Adler GK. Cardiac damage prevention by eplerenone: comparison with low sodium diet or potassium loading. *Hypertension*. 2002;39:614–618.
9. Korshunov VA, Berk BC. Smooth muscle apoptosis and vascular remodeling. *Curr Opin Hematol*. 2008;15:250–254.
10. Kraemer R. Reduced apoptosis and increased lesion development in the flow-restricted carotid artery of p75(NTR)-null mutant mice. *Circ Res*. 2002;91:494–500.
11. Rossig L, Dimmeler S, Zeiher AM. Apoptosis in the vascular wall and atherosclerosis. *Basic Res Cardiol*. 2001;96:11–22.
12. Durand E, Scoazec A, Lafont A, Boddaert J, Al HA, Addad F, Mirshahi M, Desnos M, Tedgui A, Mallat Z. In vivo induction of endothelial apoptosis leads to vessel thrombosis and endothelial denudation: a clue to the understanding of the mechanisms of thrombotic plaque erosion. *Circulation*. 2004;109:2503–2506.

13. Buus CL, Pourageaud F, Fazzi GE, Janssen G, Mulvany MJ, De Mey JG. Smooth muscle cell changes during flow-related remodeling of rat mesenteric resistance arteries. *Circ Res*. 2001;89:180–186.
14. Williams TA, Verhovez A, Milan A, Veglio F, Mulatero P. Protective effect of spironolactone on endothelial cell apoptosis. *Endocrinology*. 2006;147:2496–2505.
15. Steinberg R, Harari OA, Lidington EA, Boyle JJ, Nohadani M, Samarel AM, Ohba M, Haskard DO, Mason JC. A protein kinase Cepsilon-anti-apoptotic kinase signaling complex protects human vascular endothelial cells against apoptosis through induction of Bcl-2. *J Biol Chem*. 2007; 282:32288–32297.
16. Guo X, Chen KH, Guo Y, Liao H, Tang J, Xiao RP. Mitofusin 2 triggers vascular smooth muscle cell apoptosis via mitochondrial death pathway. *Circ Res*. 2007;101:1113–1122.
17. Tsuruta F, Masuyama N, Gotoh Y. The phosphatidylinositol 3-kinase (PI3K)-Akt pathway suppresses Bax translocation to mitochondria. *J Biol Chem*. 2002;277:14040–14047.
18. Yang L, Sun M, Sun XM, Cheng GZ, Nicosia SV, Cheng JQ. Akt attenuation of the serine protease activity of HtrA2/Omi through phosphorylation of serine 212. *J Biol Chem*. 2007;282:10981–10987.
19. Fernandez-Hernando C, Ackah E, Yu J, Suarez Y, Murata T, Iwakiri Y, Prendergast J, Miao RQ, Birnbaum MJ, Sessa WC. Loss of Akt1 leads to severe atherosclerosis and occlusive coronary artery disease. *Cell Metab*. 2007;6:446–457.
20. Hitomi H, Kiyomoto H, Nishiyama A, Hara T, Moriwaki K, Kaifu K, Ihara G, Fujita Y, Ugawa T, Kohno M. Aldosterone suppresses insulin signaling via the downregulation of insulin receptor substrate-1 in vascular smooth muscle cells. *Hypertension*. 2007;50:750–755.
21. Campbell DJ, Rong P, Kladis A, Rees B, Ganten D, Skinner SL. Angiotensin and bradykinin peptides in the TGR(mRen-2)27 rat. *Hypertension*. 1995;25:1014–1020.
22. Sander M, Bader M, Djavidani B, Maser-Gluth C, Vecsei P, Mullins J, Ganten D, Peters J. The role of the adrenal gland in hypertensive transgenic rat TGR(mREN2)27. *Endocrinology*. 1992;131:807–814.
23. Stas S, Whaley-Connell A, Habibi J, Appesh L, Hayden MR, Karuparthi PR, Qazi M, Morris EM, Cooper SA, Link CD, Stump C, Hay M, Ferrario C, Sowers JR. Mineralocorticoid receptor blockade attenuates chronic overexpression of the renin-angiotensin-aldosterone system stimulation of reduced nicotinamide adenine dinucleotide phosphate oxidase and cardiac remodeling. *Endocrinology*. 2007;148:3773–3780.
24. Wei Y, Sowers JR, Nistala R, Gong H, Uptergrove GM, Clark SE, Morris EM, Szary N, Manrique C, Stump CS. Angiotensin II–induced NADPH oxidase activation impairs insulin signaling in skeletal muscle cells. *J Biol Chem*. 2006;281:35137–35146.
25. Kroemer G, Reed JC. Mitochondrial control of cell death. *Nat Med*. 2000;6:513–519.
26. de Cavanagh EM, Inserra F, Ferder M, Ferder L. From mitochondria to disease: role of the renin-angiotensin system. *Am J Nephrol*. 2007;27: 545–553.
27. Werner ME, Chen F, Moyano JV, Yehiely F, Jones JC, Cryns VL. Caspase proteolysis of the integrin beta4 subunit disrupts hemidesmosome assembly, promotes apoptosis, and inhibits cell migration. *J Biol Chem*. 2007;282:5560–5569.
28. Montezano AC, Callera GE, Yogi A, He Y, Tostes RC, He G, Schiffrin EL, Touyz RM. Aldosterone and angiotensin II synergistically stimulate migration in vascular smooth muscle cells through c-Src-regulated redox-sensitive RhoA pathways. *Arterioscler Thromb Vasc Biol*. 2008;28: 1511–1518.
29. Llorente-Cortes V, Otero-Vinas M, Camino-Lopez S, Costales P, Badimon L. Cholesteryl esters of aggregated LDL are internalized by selective uptake in human vascular smooth muscle cells. *Arterioscler Thromb Vasc Biol*. 2006;26:117–123.
30. Sendra J, Llorente-Cortes V, Costales P, Huesca-Gomez C, Badimon L. Angiotensin II upregulates LDL receptor-related protein (LRP1) expression in the vascular wall: a new pro-atherogenic mechanism of hypertension. *Cardiovasc Res*. 2008;78:581–589.
31. Zhao W, Ahokas RA, Weber KT, Sun Y. Ang II–induced cardiac molecular and cellular events: role of aldosterone. *Am J Physiol Heart Circ Physiol*. 2006;291:H336–H343.
32. Wei Y, Whaley-Connell AT, Chen K, Habibi J, Uptergrove GM, Clark SE, Stump CS, Ferrario CM, Sowers JR. NADPH oxidase contributes to vascular inflammation, insulin resistance, and remodeling in the transgenic (mRen2) rat. *Hypertension*. 2007;50:384–391.
33. Taira M, Toba H, Murakami M, Iga I, Serizawa R, Murata S, Kobara M, Nakata T. Spironolactone exhibits direct renoprotective effects and inhibits renal renin-angiotensin-aldosterone system in diabetic rats. *Eur J Pharmacol*. 2008;589:264–271.
34. Dimmeler S, Zeiher AM. Endothelial cell apoptosis in angiogenesis and vessel regression. *Circ Res*. 2000;87:434–439.
35. Kockx MM, Muhring J, Knaapen MW, de Meyer GR. RNA synthesis and splicing interferes with DNA in situ end labeling techniques used to detect apoptosis. *Am J Pathol*. 1998;152:885–888.
36. Petrov VV, van Pelt JF, Vermeesch JR, Van D, V, Vekemans K, Fagard RH, Lijnen PJ. TGF-beta1-induced cardiac myofibroblasts are nonproliferating functional cells carrying DNA damages. *Exp Cell Res*. 2008;314: 1480–1494.
37. Patni H, Mathew JT, Luan L, Franki N, Chander PN, Singhal PC. Aldosterone promotes proximal tubular cell apoptosis: role of oxidative stress. *Am J Physiol Renal Physiol*. 2007;293:F1065–F1071.
38. Mathew JT, Patni H, Chaudhary AN, Liang W, Gupta A, Chander PN, Ding G, Singhal PC. Aldosterone induces mesangial cell apoptosis both in vivo and in vitro. *Am J Physiol Renal Physiol*. 2008;295:F73–F81.
39. De AN, Fiordaliso F, Latini R, Calvillo L, Funicello M, Gobbi M, Mennini T, Masson S. Appraisal of the role of angiotensin II and aldosterone in ventricular myocyte apoptosis in adult normotensive rat. *J Mol Cell Cardiol*. 2002;34:1655–1665.
40. Sonder SU, Woetmann A, Odum N, Bendtzen K. Spironolactone induces apoptosis and inhibits NF-kappaB independent of the mineralocorticoid receptor. *Apoptosis*. 2006;11:2159–2165.
41. Cooper SA, Whaley-Connell A, Habibi J, Wei Y, Lastra G, Manrique C, Stas S, Sowers JR. Renin-angiotensin-aldosterone system and oxidative stress in cardiovascular insulin resistance. *Am J Physiol Heart Circ Physiol*. 2007;293:H2009–H2023.
42. Shiraishi I, Melendez J, Ahn Y, Skavdahl M, Murphy E, Welch S, Schaefer E, Walsh K, Rosenzweig A, Torella D, Nurzynska D, Kajstura J, Leri A, Anversa P, Sussman MA. Nuclear targeting of Akt enhances kinase activity and survival of cardiomyocytes. *Circ Res*. 2004;94: 884–891.

On-Supplement

Mineralocorticoid Receptor Antagonism Attenuates Vascular Apoptosis and Injury via Rescuing Akt Activation

Yongzhong Wei[1,2], Adam T. Whaley-Connell[1,2], Javad Habibi[1,2], Jenna Rehmer[1,2], Nathan Rehmer[1,2], Kamlesh Patel[1], Melvin Hayden[1,2], Vincent DeMarco[1,2], Carlos M. Ferrario[4], Jamal A. Ibdah[1,3], and James R. Sowers[1,2,3]

[1]Department of Medicine and [2]Diabetes and Cardiovascular Center of Excellence, University of Missouri; [3]Harry S Truman VA Medical Center, Columbia, MO; [4]Hypertension and Vascular Disease Center, Wake Forest University School of Medicine, Winston-Salem, NC.

Running title: Aldosterone, Akt Activation and Vascular Injury

Corresponding author
James R. Sowers, MD.
Professor of Medicine, Pharmacology and physiology
Director of the Diabetes and Cardiovascular Center of Excellence
University of Missouri–Columbia
D109 Diabetes Center HSC
One Hospital Drive
Columbia, MO 65212
Phone: (573)882-2273
Fax: (573)884-5530
E-mail: sowersj@health.missouri.edu

Expanded Materials and Methods

Animals and treatments

Animal procedures were followed by the University of Missouri Animal Care and Use Committee and NIH guidelines. Male transgenic heterozygous (+/-) Ren2 rats and Sprague-Dawley (SD) littermates were received at 5-6 wk of age from Bowman Gray School of Medicine, Wake Forest University, Winston-Salem, NC. After arrival, the animals were allowed 1 week to become acclimatized to the environment, and they had free access to standard chow and tap water. The rats were randomly assigned to SD vehicle-treated (SD-C), Ren2 vehicle-treated (Ren2-C) and Ren2 spironolactone (Ren2-Sp) groups (6-7 rats/group). Rats were implanted with a subcutaneous time-release, matrix-driven delivery pellet (Innovative Research of America, Sarasota, FL) containing either spironolactone (5 mg; 0.24 mg/d) or vehicle for 21 day.[1]

Systolic Blood Pressure

Systolic blood pressure (SBP) was measured in triplicate using the tail-cuff method (Harvard Systems, Student Oscillometric Recorder) prior to and after treatment.[1]

Materials

Anti-4-Hydroxy-2-Nonenal (4-HNE) antibody was obtained from OXIS International Inc. (Portland, OR) and Alpha Diagnostic International (San Antonio, TX). Antibodies against BAD, BAD Ser^{136}, Bcl-2, and Bcl-xL were purchased from Santa Cruz Biotechnology (Santa Cruz, CA) and the antibodies against Akt, Akt Ser^{473}, Akt Thr^{308}, cytochrome c, and caspase-3 were obtained from Cell Signaling Technology (Beverly, MA). Antibodies against angiotensin II (ANG II), angiotensin type 1 receptor (AT_1R), mineralocorticoid receptor (MR), Nox2, Rac1,

p67phox, or 3- nitrotyrosine, were purchased from Santa Cruz Biotechnology (Santa Cruz, CA) and Cell Signaling Technology (Beverly, MA). *In Situ* Cell Death Detection Kit was purchased from Roche Applied Science (Indianapolis, IN).

Aorta Dissection and Protein Extraction

Aorta from arch to diaphragm was carefully dissected from the animals. The thoracic aorta was used in this investigation. The arch and top 1/3 of the thoracic aorta was removed. A 2 mm section of the aortic fragment was then removed for histological analysis and immunohistochemistry. Another 2 mm section was removed for either TEM analysis or Oil Red O staining. The remaining thoracic aorta was combined with the previously removed arch and top section of the aorta for tissue homogenization and various assay analysis. Aortic samples were homogenized in ice-cold homogenization buffer (20 mM HEPES, 10 mM KCl, 1.5 mM MgCl2, 1 mM EGTA, 1mM EDTA, 1 mM DTT, 250 mM sucrose, 0.1 mM PMSF, 2 μM leupeptin, 2 μM pepstatin A, pH 7.4) 2 mg/ml pepstatin, leupeptin, and aprotinin) using a Duall homogenizer. A portion of the whole homogenate (WH) was saved. Remaining WH was centrifuged at 800g for 10 min at 4C to remove nuclei and cell debris. The resulting supernatant (S1) was further centrifuged at 13,000g for 20 min at 4C two times, with the resulting supernatant (S2) and pellet containing mitochondria.

NADPH Oxidase Activity Assay

NADPH oxidase activity was measured as previously described.[2] Briefly, the S2 fraction (50 μg protein) from above was incubated with NADPH (100 μM) at 37^{o} C and the rate of NADPH consumption monitored by measuring the decline in absorbance (340 nm) every 10 min, using a plate reader spectrophotometer (Bio-Tek EL808).

Western Blot Analysis

To determine levels of lipid peroxidation in aortas, 4-HNE and 3-nitrotyrosine were evaluated by immunoblot. 4-HNE is a highly toxic by-product of lipid peroxidation and a sensitive marker of oxidative stress. An aliquot of S1 fractions (20 μg protein), as described above, was separated using 10% SDS-PAGE, transferred to nitrocellulose or PVDF membrane, and incubated with primary anti-4-HNE antibody (1:1000) or anti-3-nitrotyrosine (1:1000), washed, and incubated with an HRP-conjugated secondary antibody (1:10000). The signaling was captured using phosphor-imager (Bio-RAD). The intensities of the bands were quantified using Quantity One software.

To detect cytochrome c release, the mitochondria-free cytosolic fractions (S2) were prepared as above. S2 fractions containing 15 μg proteins were loaded in 12% SDS-PAGE, transferred to PVDF, probed with an anti-cytochrome c antibody (1:1000), and followed by an HRP-conjugated secondary antibody (1:10000). The intensities of the bands were quantified as described above.

To determine expression of BAD, BAD Ser^{136}, Akt, Akt Ser^{473}, caspase-3, or AT_1R, twenty μg aliquots of the S2 fractions prepared as above were separated by 10% SDS-PAGE gels, transferred to PVDF, and probed with primary antibodies (1:1000), respectively. The intensities of the bands were quantified as described above.

Immunofluorescence

Immunohistochemical staining was performed on paraffin or cryostat sections (5μm) of aortic tissue. Sections were incubated with the following antibodies: anti-BAD Ser^{136} (1:200), Bcl-2 (1:400), Bcl-xL (1:400), Akt Ser^{473} (1:200), Akt Thr^{308} (1:200), angiotensin II (ANG II) (1:200), angiotensin type 1 receptor (AT_1R) (1:200), mineralocorticoid receptor (MR) (1:200), Nox2 (1:400), Rac1 (1:400), $p67^{phox}$ (1;400), or 3-nitrotyrosine (1:400), respectively. After

washing, slides were incubated with secondary antibodies conjugated with Alex 488 or 568 or 647. Images were acquired using a Laser-Scanning confocal microscopy (Olympus IX70) and gray scale intensities were measured.

Evaluation of Apoptotic Cell Death by TUNEL

Terminal deoxynucleotidyl transferase-mediated dUTP nick end-labeling (TUNEL) assay was performed using *In Situ* Cell Death Detection Kit per manufacturer's instructions (Roche Diagnostics, Indianapolis, IN). TUNEL-positive and -negative cells were counted in 5 random fields from 5 rats/each group. Results are expressed as number of TUNEL-positive cell/total cells x 100%.

Oil Red O Staining

To determine the presence of lipid accumulation in the vasculature, Oil Red O staining was performed on frozen aortic sections. Frozen sections (5 μm) were fixed in 10% neutral buffer formalin for 10 min. after washing with distilled water; the sections were stained with Oil Red O for 15 min. The images were acquired with the Laser-Scanning confocal microscope (Olympus IX70).

Transmission Electronic Microscopy

Transmission electron microscope (TEM) was used to examine the ultrastructural changes associated vascular injury and remodeling. Aortic samples were collected and fixed in 2% glutaraldehyde/2% paraformaldehyde, and secondary fixation with 1% osmium tetroxide, embedded in Epon-Spurr's resin, sectioned at 85nm, and stained with uranyl acetate/Sato's triple lead stain. Electron microscopy was performed at University of Missouri-Columbia Electron Microscopy Core Facility using JEOL 1200-EX TEM.

Statistical Analysis

All data are reported as the means ± SEM. Dunnett's test or Student's t-test were used to determine the significance among groups. A value of $P<0.05$ was considered to be statistically significant.

1) Stas S, Whaley-Connell A, Habibi J, Appesh L, Hayden MR, Karuparthi PR, Qazi M, Morris EM, Cooper SA, Link CD, Stump C, Hay M, Ferrario C, Sowers JR. Mineralocorticoid receptor blockade attenuates chronic overexpression of the renin-angiotensin-aldosterone system stimulation of reduced nicotinamide adenine dinucleotide phosphate oxidase and cardiac remodeling. *Endocrinology.* 2007;148:3773-3780.

2) Wei Y, Sowers JR, Nistala R, Gong H, Uptergrove GM, Clark SE, Morris EM, Szary N, Manrique C, Stump CS. Angiotensin II-induced NADPH oxidase activation impairs insulin signaling in skeletal muscle cells. *J Biol Chem.* 2006;281:35137-35146.